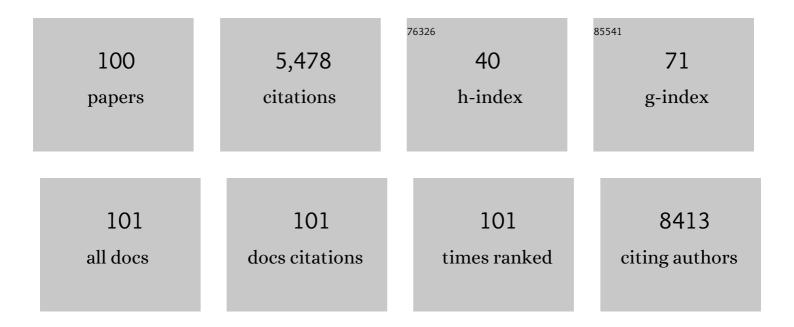
Baoyou Geng

List of Publications by Year in descending order

Source: https://exaly.com/author-pdf/4146814/publications.pdf Version: 2024-02-01



RAOVOU GENC

#	Article	IF	CITATIONS
1	Open N-doped carbon coated porous molybdenum phosphide nanorods for synergistic catalytic hydrogen evolution reaction. Nano Research, 2022, 15, 1824-1830.	10.4	35
2	Synchronous constructing ion channels and confined space of Co3O4 anode for high-performance lithium-ion batteries. Nano Research, 2022, 15, 6192-6199.	10.4	29
3	Hexamethylenetetramine induced multidimensional defects in Co ₂ P nanosheets for efficient alkaline hydrogen evolution. Chemical Communications, 2022, 58, 6352-6355.	4.1	13
4	Synergistic melamine intercalation and Zn(NO ₃) ₂ activation of N-doped porous carbon supported Fe/Fe ₃ O ₄ for efficient electrocatalytic oxygen reduction. RSC Advances, 2022, 12, 15705-15712.	3.6	4
5	Metal–Organic Framework-Derived Biln Bimetallic Oxide Nanoparticles Embedded in Carbon Networks for Efficient Electrochemical Reduction of CO ₂ to Formate. Inorganic Chemistry, 2022, 61, 12003-12011.	4.0	17
6	Constructing an interspace in MnO@NC microspheres for superior lithium ion battery anodes. Chemical Communications, 2021, 57, 10951-10954.	4.1	20
7	In Situ Electrochemical Route to Bromide Anion-Adsorbed Coral-like Porous Silver Microspheres Achieving Highly Selective Electroreduction of CO ₂ to CO over a Wide Potential Range. ACS Sustainable Chemistry and Engineering, 2021, 9, 6756-6763.	6.7	4
8	Dispersion and support dictated properties and activities of Pt/metal oxide catalysts in heterogeneous CO oxidation. Nano Research, 2021, 14, 4841-4847.	10.4	26
9	Highly dispersed Cu atoms in MOF-derived N-doped porous carbon inducing Pt loads for superior oxygen reduction and hydrogen evolution. Chemical Engineering Journal, 2021, 426, 130749.	12.7	28
10	Sandwich shelled TiO ₂ @Co ₃ O ₄ @Co ₃ O ₄ /C hollow spheres as anode materials for lithium ion batteries. Chemical Communications, 2021, 57, 1786-1789.	4.1	27
11	Self-Supported CoFe-P Nanosheets as a Bifunctional Catalyst for Overall Water Splitting. ACS Applied Nano Materials, 2021, 4, 12083-12090.	5.0	27
12	Fabrication of FeNi hydroxides double-shell nanotube arrays with enhanced performance for oxygen evolution reaction. Applied Catalysis B: Environmental, 2020, 261, 118193.	20.2	99
13	Facile one-pot synthesis of novel hierarchical Bi2O3/Bi2S3 nanoflower photocatalyst with intrinsic p-n junction for efficient photocatalytic removals of RhB and Cr(VI). Journal of Hazardous Materials, 2020, 381, 120942.	12.4	180
14	Titania supported synergistic palladium single atoms and nanoparticles for room temperature ketone and aldehydes hydrogenation. Nature Communications, 2020, 11, 48.	12.8	223
15	A multi-interfacial FeOOH@NiCo ₂ O ₄ heterojunction as a highly efficient bifunctional electrocatalyst for overall water splitting. Nanoscale, 2020, 12, 19404-19412.	5.6	38
16	Freeze-drying assisted biotemplated route to 3D mesoporous Na ₃ V ₂ (PO ₄) ₃ @NC composites as cathodes with high performance for sodium-ion batteries. Chemical Communications, 2020, 56, 11961-11964.	4.1	19
17	Pt Nanoparticles Supported on N-Doped Porous Carbon Derived from Metal–Organic Frameworks for Oxygen Reduction. ACS Applied Nano Materials, 2020, 3, 5698-5705.	5.0	27
18	Fe–Ni Layered Double Hydroxide Arrays with Homogeneous Heterostructure as Efficient Electrocatalysts for Overall Water Splitting. ACS Sustainable Chemistry and Engineering, 2019, 7, 15073-15079.	6.7	49

#	Article	IF	CITATIONS
19	Dual-Mode Long-Lived Luminescence of Mn ²⁺ -Doped Nanoparticles for Multilevel Anticounterfeiting. ACS Applied Materials & Interfaces, 2019, 11, 30146-30153.	8.0	42
20	Oxygen Vacancy–Enhanced Electrocatalytic Performances of TiO ₂ Nanosheets toward N ₂ Reduction Reaction. Advanced Materials Interfaces, 2019, 6, 1901034.	3.7	54
21	Solubility-dependent gelatination toward N-doped SnOx/C deriving from commercial SnO2 for the ultrastable lithium storage. Journal of Power Sources, 2019, 441, 227172.	7.8	13
22	Vesicular Li3V2(PO4)3/C hollow mesoporous microspheres as an efficient cathode material for lithium-ion batteries. Nano Research, 2019, 12, 1937-1942.	10.4	26
23	Heterostructural NiFe-LDH@Ni3S2 nanosheet arrays as an efficient electrocatalyst for overall water splitting. Electrochimica Acta, 2019, 318, 42-50.	5.2	84
24	Hollow porous carbon spheres doped with a low content of Co3O4 as anode materials for high performance lithium-ion batteries. Electrochimica Acta, 2019, 317, 562-569.	5.2	35
25	Simultaneous and Reversible Triggering of the Phase Transfer and Luminescence Change of Amidine-Modified Carbon Dots by CO ₂ . ACS Applied Materials & Interfaces, 2019, 11, 22851-22857.	8.0	7
26	Ultrastable and efficient H ₂ production <i>via</i> membrane-free hybrid water electrolysis over a bifunctional catalyst of hierarchical Mo–Ni alloy nanoparticles. Journal of Materials Chemistry A, 2019, 7, 16501-16507.	10.3	49
27	High-Density Pd Nanorod Arrays on Au Nanocrystals for High-Performance Ethanol Electrooxidation. ACS Applied Materials & Interfaces, 2019, 11, 20117-20124.	8.0	26
28	Defectâ€Driven Enhancement of Electrochemical Oxygen Evolution on Fe–Co–Al Ternary Hydroxides. ChemSusChem, 2019, 12, 2564-2569.	6.8	28
29	Ultrathinâ€Branched Pt Grown on Quasiâ€Sphere Pd with Enhanced Electrocatalytic Performances. ChemistrySelect, 2018, 3, 1531-1536.	1.5	0
30	Colloidal Synthesis of Mo–Ni Alloy Nanoparticles as Bifunctional Electrocatalysts for Efficient Overall Water Splitting. Advanced Materials Interfaces, 2018, 5, 1800359.	3.7	42
31	Gas template-assisted spray pyrolysis: A facile strategy to produce porous hollow Co3O4 with tunable porosity for high-performance lithium-ion battery anode materials. Nano Research, 2018, 11, 1490-1499.	10.4	45
32	Selective Reduction–Oxidation Strategy to the Conductivity-Enhancing Ag-Decorated Co-Based 2D Hydroxides as Efficient Electrocatalyst in Oxygen Evolution Reaction. ACS Sustainable Chemistry and Engineering, 2018, 6, 13420-13426.	6.7	27
33	A general gelatin-assisted strategy to hierarchical porous transition metal oxides with excellent lithium-ion storage. Electrochimica Acta, 2018, 279, 66-73.	5.2	17
34	Water Splitting Catalysts: Colloidal Synthesis of Mo-Ni Alloy Nanoparticles as Bifunctional Electrocatalysts for Efficient Overall Water Splitting (Adv. Mater. Interfaces 13/2018). Advanced Materials Interfaces, 2018, 5, 1870063.	3.7	4
35	Engineering of Hollow PdPt Nanocrystals via Reduction Kinetic Control for Their Superior Electrocatalytic Performances. ACS Applied Materials & Interfaces, 2018, 10, 29543-29551.	8.0	31
36	Morphology Engineering of Au/(PdAg alloy) Nanostructures for Enhanced Electrocatalytic Ethanol Oxidation. Particle and Particle Systems Characterization, 2018, 35, 1800258.	2.3	13

#	Article	IF	CITATIONS
37	Plasmonic Band Tunable (Au Nanocrystal)/SnO ₂ Core/Shell Hybrids for Photothermal Therapy. Particle and Particle Systems Characterization, 2018, 35, 1800238.	2.3	5
38	Atomically Dispersed Pt/Metal Oxide Mesoporous Catalysts from Synchronous Pyrolysis–Deposition Route for Water–Gas Shift Reaction. Chemistry of Materials, 2018, 30, 5534-5538.	6.7	44
39	A novel gelatin-guided mesoporous bowknot-like Co ₃ O ₄ anode material for high-performance lithium-ion batteries. Journal of Materials Chemistry A, 2017, 5, 5342-5350.	10.3	84
40	A facile and efficient strategy to gram-scale preparation of composition-controllable Ni-Fe LDHs nanosheets for superior OER catalysis. Electrochimica Acta, 2017, 225, 303-309.	5.2	46
41	Massâ€Production of Mesoporous MnCo ₂ O ₄ Spinels with Manganese(IV)―and Cobalt(II)â€Rich Surfaces for Superior Bifunctional Oxygen Electrocatalysis. Angewandte Chemie, 2017, 129, 15173-15177.	2.0	61
42	Massâ€Production of Mesoporous MnCo ₂ O ₄ Spinels with Manganese(IV)―and Cobalt(II)â€Rich Surfaces for Superior Bifunctional Oxygen Electrocatalysis. Angewandte Chemie - International Edition, 2017, 56, 14977-14981.	13.8	184
43	Scalable Dry Production Process of a Superior 3D Netâ€Like Carbonâ€Based Iron Oxide Anode Material for Lithiumâ€Ion Batteries. Angewandte Chemie, 2017, 129, 12823-12827.	2.0	21
44	Scalable Dry Production Process of a Superior 3D Netâ€Like Carbonâ€Based Iron Oxide Anode Material for Lithiumâ€Ion Batteries. Angewandte Chemie - International Edition, 2017, 56, 12649-12653.	13.8	126
45	Porous Mn ₂ O ₃ : A Low ost Electrocatalyst for Oxygen Reduction Reaction in Alkaline Media with Comparable Activity to Pt/C. Chemistry - A European Journal, 2016, 22, 9909-9913.	3.3	49
46	Self-assembled porous ceria nanostructures with excellent water solubility and antioxidant properties. RSC Advances, 2016, 6, 45957-45962.	3.6	5
47	Hydrothermal Synthesis of a rGO Nanosheet Enwrapped NiFe Nanoalloy for Superior Electrocatalytic Oxygen Evolution Reactions. Chemistry - A European Journal, 2016, 22, 14480-14483.	3.3	29
48	Mesoporous spherical Li4Ti5O12/TiO2 composites as an excellent anode material for lithium-ion batteries. Electrochimica Acta, 2016, 212, 41-46.	5.2	36
49	Facile Growth of High-Yield Gold Nanobipyramids Induced by Chloroplatinic Acid for High Refractive Index Sensing Properties. Scientific Reports, 2016, 6, 36706.	3.3	38
50	Simultaneous tunable structure and composition of PtAg alloyed nanocrystals as superior catalysts. Nanoscale, 2016, 8, 14971-14978.	5.6	40
51	Synthesis of Ag/Ag ₂ CO ₃ heterostructures with high length–diameter ratios for excellent photoactivity and anti-photocorrosion. RSC Advances, 2016, 6, 103938-103943.	3.6	9
52	Hierarchical structures composed of MnCo ₂ O ₄ @MnO ₂ core–shell nanowire arrays with enhanced supercapacitor properties. Dalton Transactions, 2016, 45, 572-578.	3.3	88
53	Excellent lithium ion storage property of porous MnCo ₂ O ₄ nanorods. RSC Advances, 2016, 6, 23074-23084.	3.6	38
54	Size-controllable synthesis of amorphous GeO _x hollow spheres and their lithium-storage electrochemical properties. RSC Advances, 2016, 6, 15952-15959.	3.6	17

#	Article	IF	CITATIONS
55	Delivery of Highly Active Nobleâ€Metal Nanoparticles into Microspherical Supports by an Aerosol‧pray Method. Chemistry - A European Journal, 2015, 21, 13291-13296.	3.3	15
56	Aerosol-spray diverse mesoporous metal oxides from metal nitrates. Scientific Reports, 2015, 5, 9923.	3.3	42
57	Au/Pt co-loaded ultrathin TiO ₂ nanosheets for photocatalyzed H ₂ evolution by the synergistic effect of plasmonic enhancement and co-catalysis. RSC Advances, 2015, 5, 98254-98259.	3.6	15
58	Superior performance asymmetric supercapacitors based on ZnCo ₂ O ₄ @MnO ₂ core–shell electrode. Journal of Materials Chemistry A, 2015, 3, 5442-5448.	10.3	158
59	Ultrathin porous nickel–cobalt hydroxide nanosheets for high-performance supercapacitor electrodes. RSC Advances, 2015, 5, 17007-17013.	3.6	62
60	Hierarchical NiMn ₂ O ₄ @CNT nanocomposites for high-performance asymmetric supercapacitors. RSC Advances, 2015, 5, 24607-24614.	3.6	73
61	Hierarchical ZnO@MnO2@PPy ternary core–shell nanorod arrays: an efficient integration of active materials for energy storage. RSC Advances, 2015, 5, 39864-39869.	3.6	15
62	Construction of unique Co ₃ O ₄ @CoMoO ₄ core/shell nanowire arrays on Ni foam by the action exchange method for high-performance supercapacitors. Journal of Materials Chemistry A, 2015, 3, 14578-14584.	10.3	84
63	Low cost visible light driven plasmonic Ag–AgBr/BiVO ₄ system: fabrication and application as an efficient photocatalyst. RSC Advances, 2015, 5, 39651-39656.	3.6	15
64	Three-dimensional NiCo ₂ O ₄ @NiMoO ₄ core/shell nanowires for electrochemical energy storage. Journal of Materials Chemistry A, 2015, 3, 12069-12075.	10.3	51
65	Well-Constructed Single-Layer Molybdenum Disulfide Nanorose Cross-Linked by Three Dimensional-Reduced Graphene Oxide Network for Superior Water Splitting and Lithium Storage Property. Scientific Reports, 2015, 5, 8722.	3.3	79
66	Ge@C core–shell nanostructures for improved anode rate performance in lithium-ion batteries. RSC Advances, 2015, 5, 17070-17075.	3.6	23
67	Facile synthesis of Fe/Ni bimetallic oxide solid-solution nanoparticles with superior electrocatalytic activity for oxygen evolution reaction. Nano Research, 2015, 8, 3815-3822.	10.4	94
68	Morphology-controllable synthesis of 3D firecracker-like ZnO nanoarchitectures for high catalytic performance. CrystEngComm, 2015, 17, 1121-1128.	2.6	13
69	ZnO nanorods/ZnSe heteronanostructure arrays with a tunable microstructure of ZnSe shell for visible light photocatalysis. Journal of Materials Chemistry A, 2014, 2, 17502-17510.	10.3	43
70	Mesocrystal precursor transformation strategy for synthesizing ordered hierarchical hollow TiO2 nanobricks with enhanced photocatalytic property. CrystEngComm, 2014, 16, 2061.	2.6	24
71	Versatile Electronic and Magnetic Properties of SnSe ₂ Nanostructures Induced by the Strain. Journal of Physical Chemistry C, 2014, 118, 9251-9260.	3.1	68
72	High supercapacitor and adsorption behaviors of flower-like MoS ₂ nanostructures. Journal of Materials Chemistry A, 2014, 2, 15958-15963.	10.3	283

#	Article	IF	CITATIONS
73	CdS urchin-like microspheres/α-Fe2O3 and CdS/Fe3O4 nanoparticles heterostructures with improved photocatalytic recycled activities. Journal of Colloid and Interface Science, 2014, 426, 83-89.	9.4	20
74	A Reliable Aerosolâ€Sprayâ€Assisted Approach to Produce and Optimize Amorphous Metal Oxide Catalysts for Electrochemical Water Splitting. Angewandte Chemie - International Edition, 2014, 53, 7547-7551.	13.8	234
75	3D porous gear-like copper oxide and their high electrochemical performance as supercapacitors. CrystEngComm, 2013, 15, 7657.	2.6	63
76	Controllable synthesis of silver nanodendrites on copper rod and its application to hydrogen peroxide and glucose detection. CrystEngComm, 2013, 15, 1173-1178.	2.6	34
77	Non-enzymatic electrochemical sensing of glucose. Mikrochimica Acta, 2013, 180, 161-186.	5.0	427
78	Shell structure-enhanced electrocatalytic performance of Au–Pt core–shell catalyst. CrystEngComm, 2013, 15, 2133.	2.6	17
79	Ag–Au bimetallic nanostructures: co-reduction synthesis and their component-dependent performance for enzyme-free H2O2 sensing. Journal of Materials Chemistry A, 2013, 1, 7111.	10.3	73
80	"Re-growth Etching―to Large-sized Porous Gold Nanostructures. Scientific Reports, 2013, 3, 2377.	3.3	19
81	A template-free route to a Fe3O4–Co3O4 yolk–shell nanostructure as a noble-metal free electrocatalyst for ORR in alkaline media. Journal of Materials Chemistry, 2012, 22, 19132.	6.7	116
82	Ni2+/surfactant-assisted route to porous α-Fe2O3 nanoarchitectures. Nanoscale, 2012, 4, 1671.	5.6	25
83	Branched twinned Au nanostructures: facile hydrothermal reduction fabrication, growth mechanism and electrochemical properties. CrystEngComm, 2012, 14, 6581.	2.6	8
84	Low-cost and highly efficient composite visible light-driven Ag–AgBr/γ-Al2O3 plasmonic photocatalyst for degrading organic pollutants. Catalysis Science and Technology, 2012, 2, 1269.	4.1	36
85	Stick-like titania precursor route to MTiO3 (M = Sr, Ba, and Ca) polyhedra. CrystEngComm, 2012, 14, 2959.	2.6	22
86	Hydrothermal route to twinned-hemisphere-like CuO architectures with selective adsorption performance. CrystEngComm, 2012, 14, 3677.	2.6	24
87	Magnetic Nanotubes: Synthesis, Properties, and Applications. Critical Reviews in Solid State and Materials Sciences, 2012, 37, 75-93.	12.3	42
88	Fabrication of ZnSe hexagonal prism with pyramid end through the chemical vapour deposition route. CrystEngComm, 2011, 13, 668-673.	2.6	3
89	A room-temperature chemical route to homogeneous core–shell Cu2O structures and their application in biosensors. CrystEngComm, 2011, 13, 697-701.	2.6	20
90	Self-assembly fabrication of 3D porous quasi-flower-like ZnO nanostrip clusters for photodegradation of an organic dye with high performance. CrystEngComm, 2011, 13, 2137.	2.6	57

#	Article	IF	CITATIONS
91	Coralloid SnO2 with hierarchical structure and their application as recoverable gas sensors for the detection of benzaldehyde/acetone. Materials Chemistry and Physics, 2010, 122, 30-34.	4.0	23
92	Facile Subsequently Light-Induced Route to Highly Efficient and Stable Sunlight-Driven Agâ^'AgBr Plasmonic Photocatalyst. Langmuir, 2010, 26, 18723-18727.	3.5	257
93	Modified Kirkendall effect for fabrication of magnetic nanotubes. Chemical Communications, 2010, 46, 1899-1901.	4.1	38
94	One-step synthesis and morphology evolution of luminescent Eu2+ doped strontium aluminate nanostructures. CrystEngComm, 2010, 12, 2722.	2.6	20
95	A facile solution chemical route to self-assembly of CuS ball-flowers and their application as an efficient photocatalyst. CrystEngComm, 2010, 12, 144-149.	2.6	157
96	Kinetic manipulation of the morphology evolution of FePO4 microcrystals: from rugbies to porous microspheres. CrystEngComm, 2009, 11, 2510.	2.6	12
97	A facile sonochemical route to morphology controlled nickel complex mesostructures. CrystEngComm, 2009, 11, 1317.	2.6	10
98	Egg albumin as a nanoreactor for growing single-crystalline Fe3O4 nanotubes with high yields. Chemical Communications, 2008, , 5773.	4.1	45
99	A facile coordination compound precursor route to controlled synthesis of Co3O4 nanostructures and their room-temperature gas sensing properties. Journal of Materials Chemistry, 2008, 18, 4977.	6.7	122
100	Perovskite phase formation, microstructure and improvement of dielectric properties in iron-containing ferroelectrics. Physica Status Solidi (A) Applications and Materials Science, 2006, 203, 2538-2545.	1.8	4